Electronic Supplementary Material (ESI) for Physical Chemistry Chemical Physics.

Supplementary Information for Excited State Energy Fluctuations in the Fenna-Matthews-Olson Complex from Molecular Dynamics Simulations with Interpolated Chromophore Potentials

Chang Woo Kim[†], *Bongsik Choi*[‡], *and Young Min Rhee*[*,‡]

[†]Department of Chemistry, Pohang University of Science and Technology (POSTECH), Pohang 37673, Korea

[‡]Department of Chemistry, Korea Advanced Institute of Science and Technology (KAIST), Daejeon 34141, Korea

Intermolecular force field of bacteriochlorophyll *a*. Because the electronic excitation in BChl *a* mainly affects the electron density near the central porphyrin moiety, we set the atomic charges of phytyl tail to be the same in the ground (S_0) and excited (S_1) electronic states. In addition, because dispersive interaction changes only negligibly with electronic excitation,[1] the dispersion parameters for the two electronic states were also set to be the same for the entire BChl *a* molecule in the two states. These parameters were already reported in ref 2. For the core part, however, more elaborate procedures were applied to reflect the atomic charge redistribution with electronic transition. (See Fig. S1 for the definition of the core part.) The atomic charges in the core part were modeled with the restrained electrostatic potential (RESP) method[3] based on QM/MM calculations to snapshots generated by MD simulations. The MM environment in these QM/MM calculations were described by the simple electrostatic embedding approach with fixed atomic point charges.[4] All the calculations were performed with Q-Chem 4.3[5] and GROMACS 4.5[6] packages.

Fig. S1 The core part of the BChl *a* molecule after truncating the phytyl tail. Atomic charges on these atoms were fit with RESP in a state-specific manner. The interpolation region was somewhat smaller and is denoted with thick sticks.

As a preparation step, the ground state vacuum RESP charges were evaluated and used as initial guess for collecting the system snapshots for refining QM/MM calculations. For this purpose, the atomic coordinates of the third pigment (Site 3) were taken from the crystal structure (PBD ID: 3BSD)[7] and its phytyl tail was replaced by a hydrogen atom to form the core part. Figure S1 was actually drawn with this structure. Site 3 was chosen because its sidechains are the least congested among the seven pigment molecules, thus minimizing the ambiguity in RESP fitting caused by buried atoms. We optimized this molecular geometry in the vacuum by using at the B3LYP/6-31G(d,p) level, and then fitted the atomic charges by using the electrostatic potential generated at the optimized geometry.[3] The set of RESP charges thus obtained were used for all seven pigment sites for obtaining refined charges. By following the same procedures described in Section 2 of the main text, the system was first subjected to 1 ns of MD for equilibration and then to additional 10 ns for production at 300 K and 1 bar. The atomic positions were saved every 10 ps during the production run. The RESP charges were evaluated again for the 1000 collected snapshots by using the electrostatic potential from QM/MM calculations. Of course, the QM region was the core part of BChl *a*. To prevent over-polarization of the QM region, the atomic charges of the CH_2 MM moiety covalently bonded to the core part were set to zero. The final atomic charge values for the ground state were determined as the average of the 1000 sets of RESP charges. This process was repeated for all seven pigments.

In principle, the method described in the above can be straightforwardly extended to refining excited state atomic charges. However, simply repeating the same procedure for the excited state is unlikely to give the best description of electrostatics for our purpose for various reasons. For example, the functional form of electrostatic interaction exerted by an MM atom is different between IM/MM and QM/MM (force- shifted Coulomb versus finite cutoff). In the end, the purpose of IM/MM is to closely mimic its reference QM/MM[8] and in this work, the gap energy

between electronic states is important. Thus, we designed a different fitting procedure that is optimized toward reproducing the gap energy.

Let us denote the IM/MM excitation energy of the full system as $\Delta E_{\mathrm{IM/MM}}$ and that of the interpolation region in vacuum as ΔE_{IM}. The "Δ" sign here stresses that it denotes the gap energy. The change in the excitation energy of the IM region by its environment, $\Delta\Delta E_{\mathrm{IM\text{-}env}}$, is the difference between the two excitation energies:

$$\Delta\Delta E_{\mathrm{IM\text{-}env}} = \Delta E_{\mathrm{IM/MM}} - \Delta E_{\mathrm{IM}} \tag{S1}$$

In our IM/MM simulation scheme, the bonded interaction outside the interpolation region is identical for the ground and the excited states and does not contribute to $\Delta E_{\mathrm{IM/MM}}$.[9] Under such condition $\Delta\Delta E_{\mathrm{IM\text{-}env}}$ is strictly equal to the electrostatic contribution to the excitation energy, and it solely depends on the atomic charges that we are trying to refine. Meanwhile, the environment-induced change of quantum chemically calculated excitation energy $\Delta\Delta E_{\mathrm{QM\text{-}env}}$ is defined analogously to eqn (S1), namely

$$\Delta\Delta E_{\mathrm{QM\text{-}env}} = \Delta E_{\mathrm{QM/MM}} - \Delta E_{\mathrm{QM}} \tag{S2}$$

where $\Delta E_{\mathrm{QM/MM}}$ is evaluated by setting the QM region to be the BChl *a* core part. As ΔE_{IM} already matches quite well with ΔE_{QM},[9] to make the two gap energies ($\Delta E_{\mathrm{IM/MM}}$ and $\Delta E_{\mathrm{QM/MM}}$) agree with each other, we need to parameterize such that $\Delta\Delta E_{\mathrm{IM\text{-}env}}$ closely mimics $\Delta\Delta E_{\mathrm{QM\text{-}env}}$. The next scheme visualizes this plan in a pictorial way.

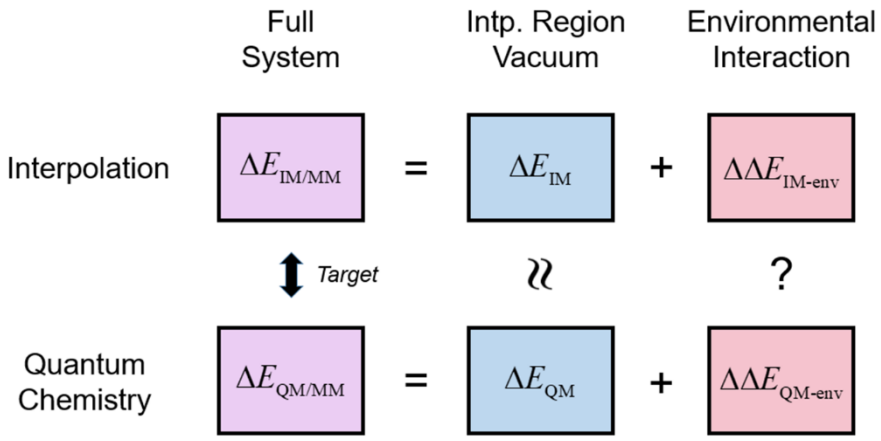

Scheme S1 Diagrammatic representation of the charge fitting scheme for the excited state. We are targeting to reproduce the QM/MM excitation energy for the full system (purple) with IM/MM. Because the full interaction term can be decomposed into contributions by a vacuum term (blue) and an environmental interaction term (red), and because the agreement in the vacuum term has already been established in ref 9, we need to pursue matching the environmental interaction.

The optimization of the excited state atomic charges was practically attained by minimizing the mean square error between $\Delta\Delta E_{\mathrm{IM\text{-}env}}$ and $\Delta\Delta E_{\mathrm{QM\text{-}env}}$ based on 1000 snapshots collected for refining ground state atomic charges. $\Delta\Delta E_{\mathrm{QM\text{-}env}}$ was evaluated at the TD-B3LYP/6-31G(d,p) level. The excited state atomic charges were optimized[10] with a constraint that the sum of the charges is zero. The optimization was initiated after setting the charges to the refined ground state values. This procedure was repeated for all seven pigments. Figure S2 displays how the agreement between $\Delta\Delta E_{\mathrm{IM\text{-}env}}$ and $\Delta\Delta E_{\mathrm{QM\text{-}env}}$ improves with our scheme. Of course, the agreement is not perfect due to the limitation of the fixed point charge model, but the improvement is noticeable. Also, the errors are mostly less than 0.1 eV, which is definitely better than the accuracy level of commonly adopted TDDFT approaches.

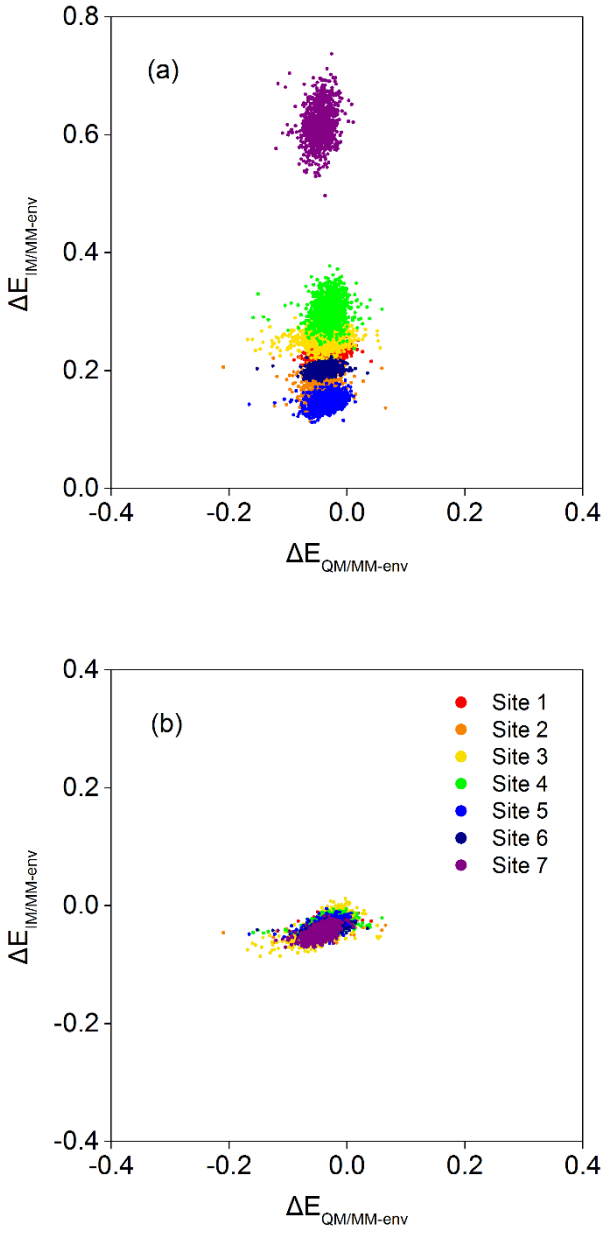

Fig. S2 Comparison between $\Delta\Delta E_{\text{IM-env}}$ and $\Delta\Delta E_{\text{QM-env}}$ with (a) excited state atomic charges from simple RESP and (b) by the fitting process in Scheme S1.

TrESP point charges of bacteriochlorophyll *a* molecule. For each of the 1000 snapshots adopted for generating state-dependent atomic partial charges as described in the above, the transition density between the ground and the excited states was evaluated by QM/MM with TD-B3LYP/6-31G(d,p). Again, the TrESP charges were averaged over the whole set of snapshots.

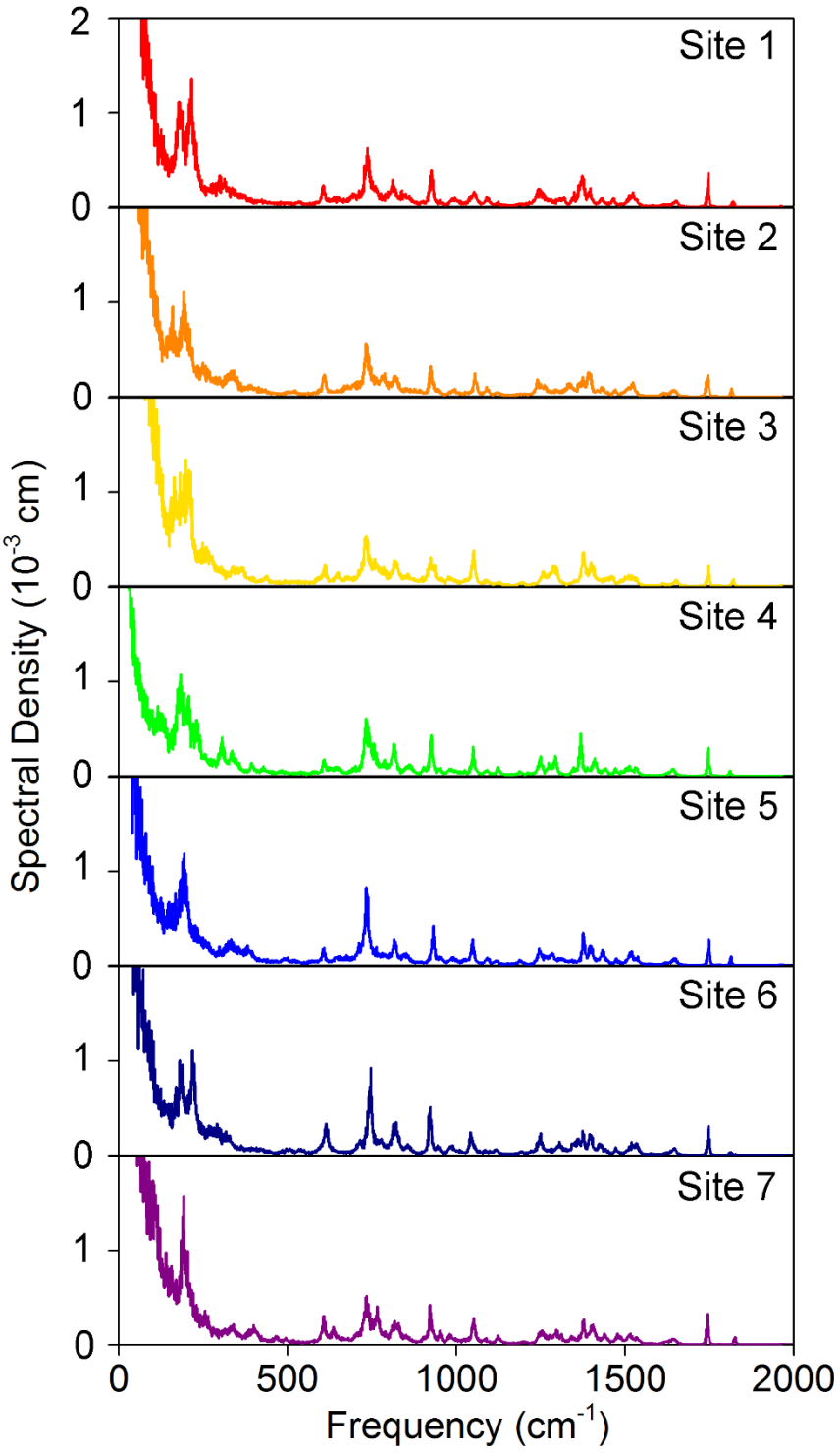

Fig. S3 The complete set of spectral densities for the seven pigment sites in the FMO complex in the scaled form, $J(\omega)/\omega^2$.

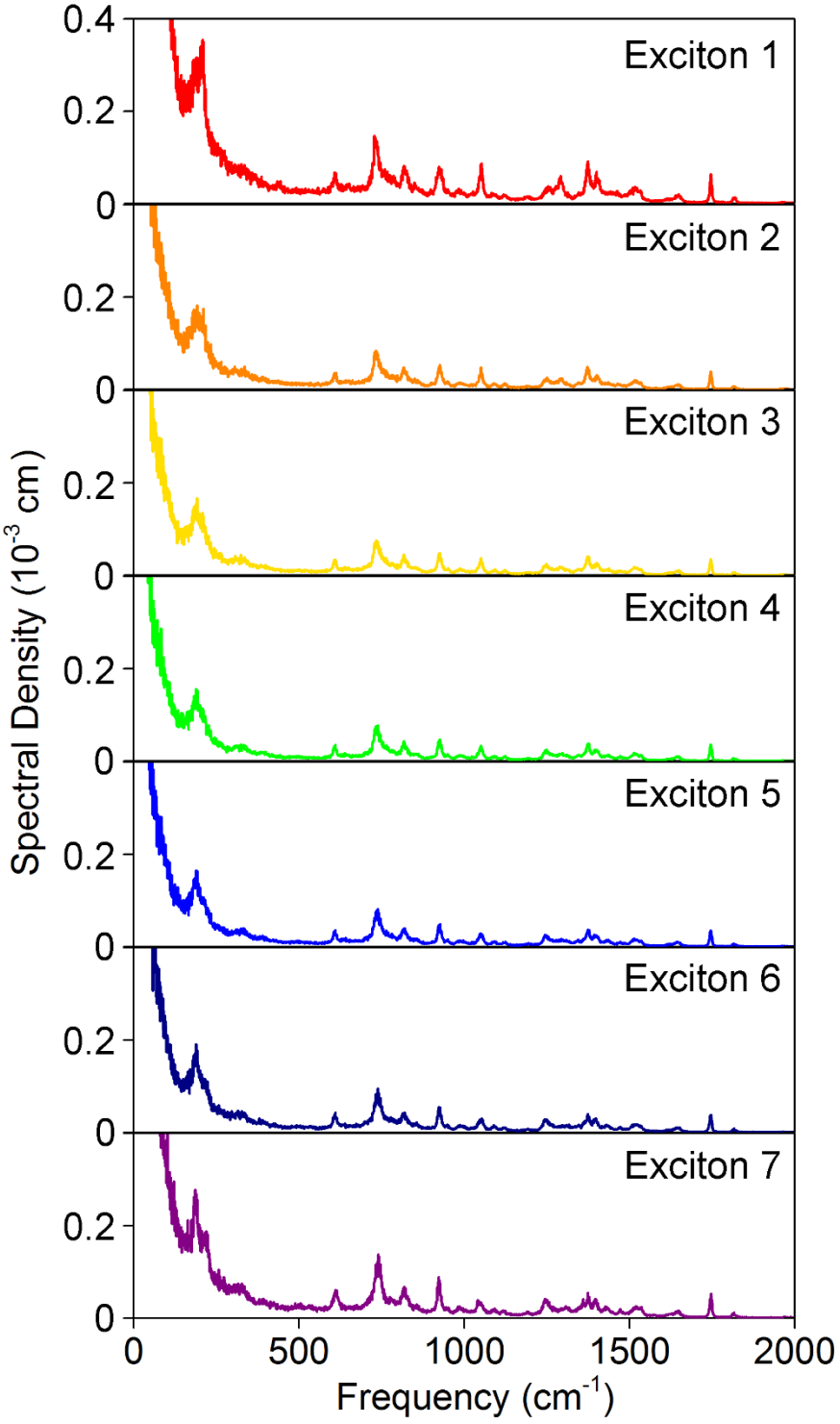

Fig. S4 The complete set of spectral densities for the seven adiabatic exciton states of the FMO complex in the scaled form, $J(\omega)/\omega^2$.

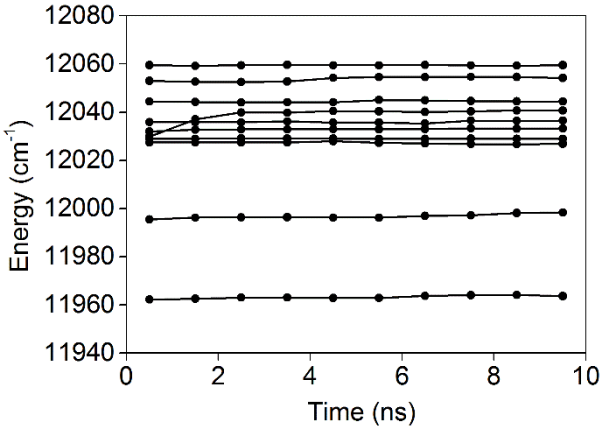

Fig. S5 Drifts of the lowest exciton energies in time from 4.5 K simulations. In each trajectory, the energies were time averaged over 1 ns windows to eliminate fluctuations from fast dynamic disorder.

Supplementary References

1. C.-I. Song and Y. M. Rhee, *Int. J. Quantum Chem.*, 2011, **111**, 4091-4105.
2. M. Ceccarelli, P. Procacci and M. Marchi, *J. Comp. Chem.*, 2003, **24**, 129-142.
3. C. I. Bayly, P. Cieplak, W. Cornell and P. A. Kollman, *J. Phys. Chem.*, 1993, **97**, 10269-10280.
4. A. Warshel and M. Levitt, *J. Mol. Biol.*, 1976, **103**, 227-249.
5. Y. Shao, Z. Gan, E. Epifanovsky, A. T. B. Gilbert, M. Wormit, J. Kussmann, A. W. Lange, A. Behn, J. Deng, X. Feng, D. Ghosh, M. Goldey, P. R. Horn, L. D. Jacobson, I. Kaliman, R. Z. Khaliullin, T. Kuś, A. Landau, J. Liu, E. I. Proynov, Y. M. Rhee, R. M. Richard, M. A. Rohrdanz, R. P. Steele, E. J. Sundstrom, H. L. Woodcock, P. M. Zimmerman, D. Zuev, B. Albrecht, E. Alguire, B. Austin, G. J. O. Beran, Y. A. Bernard, E. Berquist, K. Brandhorst, K. B. Bravaya, S. T. Brown, D. Casanova, C.-M. Chang, Y. Chen, S. H. Chien, K. D. Closser, D. L. Crittenden, M. Diedenhofen, R. A. DiStasio, H. Do, A. D. Dutoi, R. G. Edgar, S. Fatehi, L. Fusti-Molnar, A. Ghysels, A. Golubeva-Zadorozhnaya, J. Gomes, M. W. D. Hanson-Heine, P. H. P. Harbach, A. W. Hauser, E. G. Hohenstein, Z. C. Holden, T.-C. Jagau, H. Ji, B. Kaduk, K. Khistyaev, J. Kim, J. Kim, R. A. King, P. Klunzinger, D. Kosenkov, T. Kowalczyk, C. M. Krauter, K. U. Lao, A. D. Laurent, K. V. Lawler, S. V. Levchenko, C. Y. Lin, F. Liu, E. Livshits, R. C. Lochan, A. Luenser, P. Manohar, S. F. Manzer, S.-P. Mao, N. Mardirossian, A. V. Marenich, S. A. Maurer, N. J. Mayhall, E. Neuscamman, C. M. Oana, R. Olivares-Amaya, D. P. O'Neill, J. A. Parkhill, T. M. Perrine, R. Peverati, A. Prociuk, D. R. Rehn, E. Rosta, N. J. Russ, S. M. Sharada, S. Sharma, D. W. Small, A. Sodt, T. Stein, D. Stück, Y.-C. Su, A. J. W. Thom, T. Tsuchimochi, V. Vanovschi, L. Vogt, O. Vydrov, T. Wang, M. A. Watson, J. Wenzel, A. White, C. F. Williams, J. Yang, S. Yeganeh, S. R. Yost, Z.-Q. You, I. Y. Zhang, X. Zhang, Y. Zhao, B. R. Brooks, G. K. L. Chan, D. M. Chipman,

C. J. Cramer, W. A. Goddard, M. S. Gordon, W. J. Hehre, A. Klamt, H. F. Schaefer, M. W. Schmidt, C. D. Sherrill, D. G. Truhlar, A. Warshel, X. Xu, A. Aspuru-Guzik, R. Baer, A. T. Bell, N. A. Besley, J.-D. Chai, A. Dreuw, B. D. Dunietz, T. R. Furlani, S. R. Gwaltney, C.-P. Hsu, Y. Jung, J. Kong, D. S. Lambrecht, W. Liang, C. Ochsenfeld, V. A. Rassolov, L. V. Slipchenko, J. E. Subotnik, T. Van Voorhis, J. M. Herbert, A. I. Krylov, P. M. W. Gill and M. Head-Gordon, *Mol. Phys,*, 2015, **113**, 184-215.

6. S. Pronk, S. Páll, R. Schulz, P. Larsson, P. Bjelkmar, R. Apostolov, M. R. Shirts, J. C. Smith, P. M. Kasson, D. van der Spoel, B. Hess and E. Lindahl, *Bioinformatics*, 2013, **29**, 845-854.
7. A. Ben-Shem, F. Frolow and N. Nelson, *FEBS Lett.*, 2004, **564**, 274-280.
8. J. W. Park and Y. M. Rhee, *ChemPhysChem*, 2014, **15**, 3183-3193.
9. C. W. Kim and Y. M. Rhee, *J. Chem. Theory Comput.*, 2016, **12**, 5235-5246.
10. R. Fletcher, *Practical Methods of Optimization*, Wiley, 1987.